ELSEVIER

Polymer 40 (1999) 3323–3329

polymer

Structural analysis of core-shell type polymer particles composed of poly(butyl acrylate) and poly(methyl methacrylate) by high-resolution solid-state ^{13}C n.m.r. spectroscopy

Masato Ishida[a], Junji Oshima[a], Kunio Yoshinaga[a], Fumitaka Horii[b,*]

[a]*Takeda Chemical Industries, Yodogawa, Osaka 532, Japan*
[b]*Institute for Chemical Research, Kyoto University, Uji, Kyoto 611, Japan*

Received 9 March 1998; received in revised form 22 May 1998; accepted 13 July 1998

Abstract

The phase-separated structure and molecular mobility for core-shell type polymer particles composed of poly(butyl acrylate) (PBA) and poly(methyl methacrylate) (PMMA) have been examined by high-resolution solid-state ^{13}C n.m.r. spectroscopy. These types of polymer particles were prepared by the two-step emulsion polymerization of BA and MMA in the presence or absence of ally methacrylate (AMA) as a crosslinking agent. The analysis of the $^{1}H-^{13}C$ cross polarization process has revealed that molecular mobility of the main-chain of PBA is significantly restricted for sample BA2M prepared in the presence of 1.6 wt% AMA. ^{1}H spin–lattice relaxation time measurements in the rotating frame have also revealed that the PBA and PMMA phases are phase-separated in a scale of several nm for the polymer particles. Furthermore, the ^{1}H spin diffusion process, measured by the combined pulse sequence of the Goldman–Shen pulse sequence and the CP process, has been successfully analyzed in terms of the equation derived by the simple two-spin cross relaxation theory. The time constant T_{SD} for the ^{1}H spin diffusion between two polymers obtained through this analysis has been found to be a useful parameter to elucidate the phase-separated structure. On the basis of these results, it is concluded that the PBA/PMMA polymer particles have a rather incompletely phase-separated core-shell type structure but the addition of an appropriate amount of AMA improves such a structure by confining the distribution of PMMA domains around the surface of the polymer particles probably as a result of the preferential crosslinking in the PBA phase.

Keywords: Core-shell type polymer particles; CP-MAS ^{13}C n.m.r.; Phase-separated structure

1. Introduction

It is well known that core-shell type polymer particles, which are composed of rubbery cores and rigid shells, improve the impact strength of thermoplastic resins when they are mixed with the resins [1]. In particular, the core-shell type polymer particles that are composed of poly(butyl acrylate) (PBA) cores and poly(methyl methacrylate) (PMMA) shells are found to be very effective for the improvement of the impact strength for thermoplastic resins [2,3] and for the relaxation of the residual stress for thermosetting resins [4,5]. To further improve the practical characteristics of these polymer particles, it is very important to characterize the core-shell structure in detail.

Until now, many investigations of the core-shell structure have been performed by using various analytical methods, such as differential scanning calorimetry (DSC) [6,7], dynamic mechanical analysis (DMA) [7,8] transmission electron microscopy (TEM) [9–11], X-ray photoelectron spectroscopy (XPS) [12], infrared spectroscopy (IR) [13], nuclear magnetic resonance (n.m.r.) [14], and gel permeation chromatography (GPC) [15]. However, the detailed core-shell structure and the compatibility in the interphase between the core and the shell, including the effects of crosslinking agents, have not been clarified well yet.

High-resolution solid-state ^{13}C n.m.r. spectroscopy is very powerful in characterizing the phase-separated structure for crystalline polymers [16–21], polyurethanes [16,22,23], polymer blends [16,24], etc. As for core-shell type polymer particles, Spiess et al. extensively investigated their phase-separated structure by one- and two-dimensional solid-state n.m.r. methods [25–27]. For example, they clarified the difference in morphology between core-shell type polymer particles synthesized at high and low temperatures: the low-temperature polymer particles have an interface with a continuous concentration gradient of two

* Corresponding author.

0032-3861/99/$ - see front matter
PII: S0032-3861(98)00541-2

components mixed on a molecular level, whereas the interface of the high-temperature particles with almost the same thickness is composed of micro phase-separated domains.

In this paper, we have examined the phase-separated structure and compatibility for core-shell type polymer particles which were synthesized by the two-step emulsion polymerization of butyl acrylate (BA) and methyl methacrylate (MMA) in the presence or absence of allyl methacrylate (AMA) as a crosslinking agent by solid-state ^{13}C n.m.r. spectroscopy. In particular, the effect of the crosslinking agent on the phase-separated structure has been elucidated by analyzing the ^{1}H spin diffusion process.

2. Experimental

2.1. Materials

Table 1 lists monomer compositions of BA, MMA and AMA for three types of core-shell polymer particles, which are coded as BM, BA1M and BA2M in this study. Each emulsion was prepared in the presence of sodium persulfate as a polymerization initiator and dioctyl sodium sulfosuccinate as an emulsifier. The synthesis of core-shell polymer particles was carried out by the seed emulsion polymerization at 70°C. At the first step, the seed particles with about 90 nm in diameter were prepared by polymerizing 4 wt% of the core monomer. The polymerization was continued by step-wise adding of an appropriate amount of emulsion which was a mixture of the core monomer, the emulsifier, and deionized water. At the end of the first-step polymerization, we confirmed the two following points: (1) the polymerization conversion is more than 99%; (2) the particle size of the core is not much different from the value (225 nm) expected in the ideal seed emulsion polymerization. The second polymerization was initiated by adding first the initiator and then by step-wise adding another emulsion containing the shell monomer. Finally the polymerization conversion was also confirmed to be more than 99%. In this study, each polymerization conversion was estimated from the weight of each specimen dried at 110°C, and the particle size was measured by means of dynamic light scattering. The core-shell polymer particles thus prepared were separated from the polymerization system by the freeze-drying method.

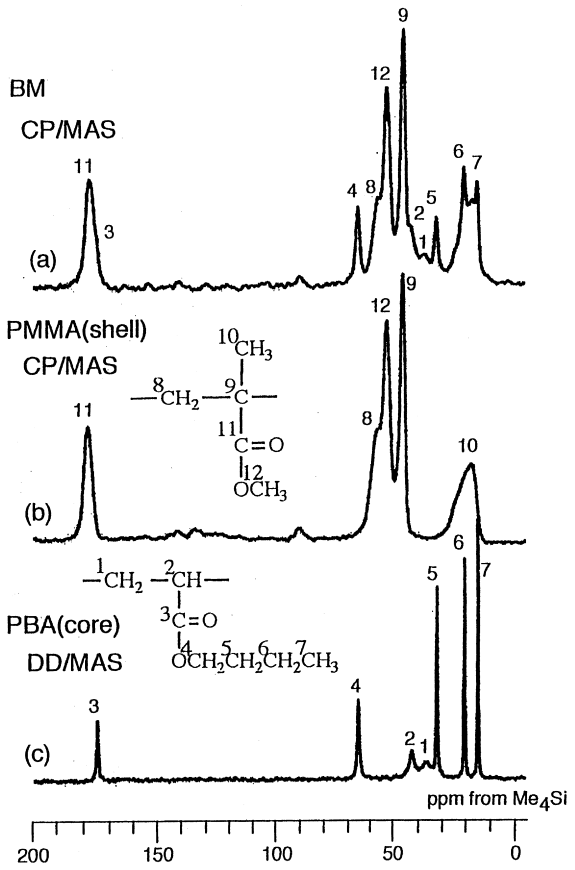

Fig. 1. 67.8 MHz ^{13}C n.m.r. spectra measured at 30°C: (a) and (b) by CP/MAS, (c) by DD/MAS.

2.2. Solid-state ^{13}C n.m.r. measurements

Solid-state ^{13}C n.m.r. measurements were performed on a JEOL JNM-EX270 spectrometer equipped with a variable temperature MAS system operating at 67.8 MHz under a static magnetic field of 6.35 T. Each dried sample was packed into a 6 mm diameter zirconia rotor. ^{1}H 90° pulse width was 4.0 μs and the CP contact time was 2.0 ms except for measurements of the CP process. The number of scans was about 500, but it was increased up to about 2000 in ^{1}H spin diffusion experiments. The MAS rate was set to 5 kHz and the pulse recycle time was 5 s. Dipolar decoupled/MAS (DD/MAS) ^{13}C n.m.r. spectra were also measured for the rubbery polymer (PBA) by using the $\pi/4$ single pulse sequence instead of the CP excitation. ^{13}C chemical shifts were expressed as values

Table 1
Monomer compositions for the preparation of the different core-shell polymer particles

Sample	Core		Shell	
	Monomer	Mole fraction	Monomer	Mole fraction
BM	BA	0.8	MMA	0.20
BA1M	BA/AMA	0.7984/0.0016	MMA	0.20
BA2M	BA/AMA	0.784/0.016	MMA	0.20

relative to tetramethylsilane (Me_4Si) by using the CH_3 line at 17.36 ppm of hexamethylbenzene crystals as an external reference.

3. Results and discussion

3.1. CP/MAS and DD/MAS ^{13}C n.m.r. spectra

Fig. 1 shows high-resolution solid-state ^{13}C n.m.r. spectra of the core-shell polymer particles BM, PBA homopolymer and PMMA homopolymer, which were measured at 30°C by CP/MAS or DD/MAS spectroscopy. The assignment of each resonance line has been made on the basis of the results of the solution-state spectra as well as the quaternary carbon-enhanced spectra obtained by the dipolar diphasing method [28]. As is seen in Fig. 1(a), the resonance lines for the C1 and C2 carbons in the main chain of PBA are very weak compared with those for the side-chain carbons. Accordingly, we deal with the resonance lines of the side-chain carbons of PBA for further investigations.

It is found from Fig. 1 that the chemical shifts of the core-shell polymer particles are not different from those of the constituent homopolymers. Further, there are also no differences in line width and chemical shift among samples BM, BA1M and BA2M. These facts indicate that almost no information about crosslinking and the phase-separated structure of the core-shell polymer particles may be obtainable from these spectra. Next we have measured several kinds of magnetic relaxation times.

3.2. ^{13}C spin–lattice relaxation times

In order to characterize the solid structure of polymers, ^{13}C spin–lattice relaxation times (T_{1C}) are frequently measured by means of the high-resolution solid-state n.m.r. methods. Table 2 lists T_{1C} values of the respective resonance lines measured for the three samples by the CPT1 pulse sequence [29]. It is evidently found in Table 2 that the difference of the structure, which may be produced by the introduction of crosslinking points composed of AMA residues, is hardly reflected on the T_{1C} values in these core-shell type polymer particles.

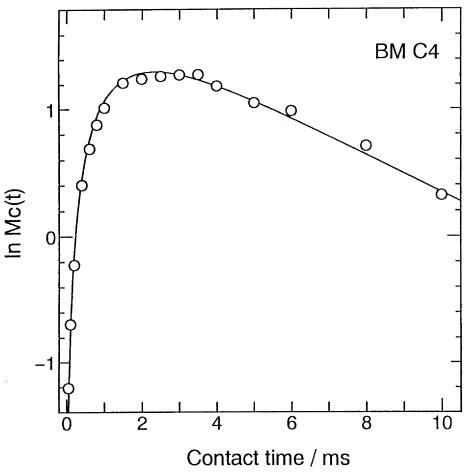

Fig. 2. CP process for the resonance line of the C4 carbon for sample BM, measured at 30°C. The solid line is the result simulated by Eq. (1).

3.3. Cross polarization process

According to the simple theory for the CP process [30,31], the ^{13}C magnetization $M_c(t)$ enhanced through this process is expressed as a function of the contact time t when $T_{CH} \ll T_{1\rho H} < T_{1\rho C}$:

$$M_c(t) = M_e[\exp(-t/T_{1\rho H}) - \exp(-t/T_{CH})] \quad (1)$$

Here, M_e is the ^{13}C equilibrium magnetization obtained when both spin systems fully contact each other without any energy exchange with the lattice, T_{CH} is the time constant for the energy exchange between ^1H and ^{13}C spin systems, and $T_{1\rho H}$ and $T_{1\rho C}$ are the ^1H and ^{13}C spin–lattice relaxation times in the rotating frames, respectively. This equation indicates that the ^{13}C magnetization appears at the rate of the order of $(T_{CH})^{-1}$ and disappears at the rate of $(T_{1\rho H})^{-1}$.

Fig. 2 shows a semilogarithmic plot of the peak intensity as a function of the contact time t for the C4 carbon of sample BM. The solid curve indicates the theoretical result based on Eq. (1) obtained by the computer-aided least-squares method. The experimental data seem to be in good accord with the theoretical curve, although the simple theory described above may not fully hold in those samples with complicated phase-separated structures. Similar good

Table 2
T_{1C} values of the respective carbons of different samples measured by the CPT1 pulse sequence at 30°C

		BM	BA1M	BA2M
PMMA	C9	8.2	8.4	8.5
	C11	15.3	15.2	15.6
	C12	10.7	10.8	11.2
PBA	C4	0.26	0.27	0.26
	C5	0.41	0.41	0.40
	C6	0.52	0.55	0.53
	C7	1.72	1.68	1.75

Table 3
Time constants (T_{CH}) for the energy exchange between ^{1}H and ^{13}C spin systems and ^{1}H spin–lattice relaxation times ($T_{1\rho H}$) in the rotating frame, which were obtained by the analysis of the CP process for each sample at 30°C

	T_{CH} (ms)			$T_{1\rho H}$ (ms)		
	C4	C5	C9	C4	C5	C9
BM	1.17	0.67	0.38	6.8	> 50	12
BA1M	1.22	0.70	0.36	6.8	> 50	11
BA2M	0.70	0.72	0.40	5.4	43	11

accordances could be obtained for the C4, C5 and C9 carbons in BM as well as for the corresponding carbons of BA1M and BA2M. The T_{CH} and $T_{1\rho H}$ values thus obtained are listed in Table 3. As for T_{CH} values for BM and BA1M, there are almost no differences for the respective carbons between these two samples.

In contrast, the T_{CH} value of the C4 carbon of BA2M is markedly shorter than the corresponding T_{CH} values for BM and BA1M, while the T_{CH} values of the C5 and C9 carbons are almost the same for these three samples. This fact indicates that the effect of the introduction of crosslinking by AMA units appears mainly for the C4 carbon, which is the most neighboring side-chain carbon to the main chain, possibly as a result of the reduction in molecular mobility of the main chain by crosslinking. It should be, therefore, noted that T_{CH} values are very sensitive for crosslinking in the rubbery state.

3.4. ^{1}H and ^{13}C spin–lattice relaxation times in the rotating frames

In the characterization of the mixing state in the several nm scale for polymer blends, $T_{1\rho H}$ values of the component polymers are frequently measured because these values reflect such a mixing state as a result of averaging of the relaxation through the ^{1}H spin diffusion between those polymers during the period corresponding to $T_{1\rho H}$. Table 4 lists the $T_{1\rho H}$ values of the respective carbons of sample BM, which were measured at 30° and − 40°C by using the standard pulse sequence for $T_{1\rho H}$ measurements equipped in the JEOL n.m.r. system. It should be first noted that the $T_{1\rho H}$ values at 30°C thus obtained for PBA are significantly different from the corresponding values in Table 3 obtained by the analysis of the CP process. The cause of the discordance is not clear at present but the $T_{1\rho H}$ values indirectly determined may contain some unknown contribution in the CP process particularly for the rubbery component. It seems, therefore, plausible to discuss relative changes in $T_{1\rho H}$ instead of the absolute values, as done in the previous section.

As is clearly seen in Table 4, the $T_{1\rho H}$ values for PMMA are greatly different from those for PBA at 30°C. This fact indicates that the ^{1}H spin diffusion between the two polymers is very slow compared with the order of $(T_{1\rho H})^{-1}$. It is, however, impossible to conclude that this sample is really phase-separated in a scale of several nm, because the ^{1}H spin diffusion may be simply slow at 30°C due to the enhanced molecular motion in the rubbery state. Therefore, we have measured the $T_{1\rho H}$ values at − 40°C, where PBA is also in the glassy state ($T_g \fallingdotseq -30$°C [32]). The $T_{1\rho H}$ values at − 40°C are also shown in Table 4. The $T_{1\rho H}$ values for PMMA are in good agreement with those for PBA. In contrast, $T_{1\rho C}$ values for PMMA and PBA in sample BM, which were measured by the standard pulse sequence for $T_{1\rho C}$ measurements and are also shown in Table 4, are significantly different from each other at − 40°C. The latter fact indicates that the molecular mobility should be appreciably different between PMMA and PBA at − 40°C. This finding further leads to the interpretation that the agreement of $T_{1\rho H}$ values between PMMA and PBA should be realized through their efficient ^{1}H spin diffusion. It is, therefore, concluded that most of PMMA and PBA are compatible in sample BM in a scale of several nm; the PMMA domain with several nm may be dispersed in the PBA continuous phase. Since similar agreements of the $T_{1\rho H}$ values were also obtained at − 40°C for samples BA1M and BA2M, it was very difficult

Table 4
$T_{1\rho H}$ and $T_{1\rho C}$ values of the respective resonance lines of sample BM, measured at 30° and − 40°C

		30°C	− 40°C	
		$T_{1\rho H}$ (ms)	$T_{1\rho H}$ (ms)	$T_{1\rho C}$ (ms)
PMMA	C9	15.4	6.2	20.7
	C12	15.7	6.1	21.3
PBA	C2	–	6.1	12.8
	C4	2.8	6.2	3.9
	C5	3.0	6.1	4.9
	C6	3.0	6.0	4.5
	C7	3.2	6.4	13.3

–Not observed clearly.

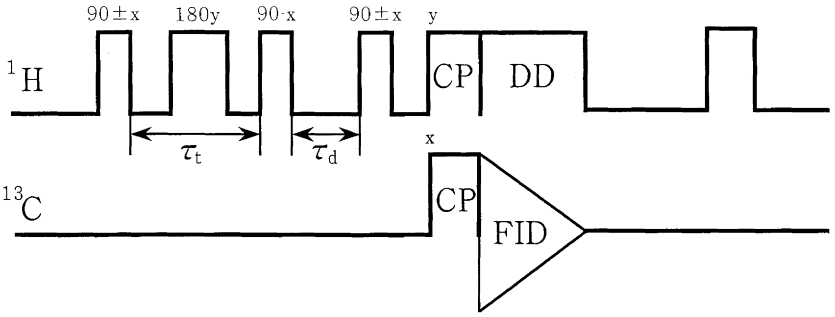

Fig. 3. Pulse sequence combined with the Goldman–Shen pulse sequence and the cross polarization technique.

to characterize the difference in phase-separated structure among these samples by using these $T_{1\rho H}$ values.

3.5. ^{1}H spin diffusion measurements

To examine the phase-separated structure for the core-shell type polymer particles in more detail, the ^{1}H spin diffusion process has been measured at 30°C by the pulse sequence shown in Fig. 3.

This pulse sequence has been prepared by the combination of the Goldman–Shen pulse sequence [33] and the CP technique [24]. In this measurement, the concentration gradient of the ^{1}H magnetization should be produced by using the difference in ^{1}H spin–spin relaxation time (T_{2H}). This condition is fulfilled for the core-shell polymer particles, since these materials are composed of the rubbery PBA and glassy PMMA components. The detailed descriptions of the pulse sequence are as follows: in the first step ^{1}H, magnetization of PBA is left as a long T_{2H} component. Next, the ^{1}H spin diffusion and the ^{1}H spin–lattice relaxation are allowed to proceed during the τ_d period. After that period, the ^{1}H magnetization in each phase-separated region is transferred to the corresponding ^{13}C spin system through CP and finally the ^{1}H spin diffusion process is detected as the change in ^{13}C magnetization as a function of τ_d. In this pulse sequence, the ^{1}H magnetization is alternately flipped to the z and $-z$ axes during the τ_d period to reduce the effect of the ^{1}H spin–lattice relaxation.

Fig. 4 shows ^{13}C n.m.r. spectra of BM in the frequency range of 0–90 ppm, which were measured by the pulse sequence shown in Fig. 3. At $\tau_d = 1$ four resonance lines assignable to the side-group carbons of PBA are clearly observed as a result of the suppression of the contribution from PMMA. However, with increasing τ_d value, the resonance lines are abruptly increased in intensity and finally tend to disappear, indicating the real occurrence of the ^{1}H spin diffusion from the PBA domains to the PMMA domains in concomitance with the ^{1}H spin–lattice relaxation. In addition, all resonance lines ascribed to PMMA or PBA are respectively increased or decreased at the same rate, suggesting that the ^{1}H spin diffusion in each domain is very rapid compared with the ^{1}H spin diffusion between the PMMA and PBA domains. In Fig. 5 the logarithmic peak intensities for the resonance line of the C12 carbon shown in Fig. 4 are plotted against the diffusion time τ_d as a representative example. The steep initial increase will be due to the ^{1}H spin diffusion from the PBA domains, while the relatively slow decay may be ascribed to the ^{1}H spin–lattice relaxation process.

To analyze such a change of the ^{1}H magnetization in this system, we assume the energy exchange process associated with ^{1}H spins as shown in Fig. 6. Here, ^{1}H spin systems for PBA and PMMA are connected with each other through the ^{1}H spin diffusion with the time constant T_{SD}. The PBA and PMMA spin systems are also connected with the lattice with the spin–lattice relaxation times T_{1HR} and T_{1HG}, respectively. As confirmed experimentally (cf. Fig. 4), the ^{1}H magnetization is homogeneous in each spin system due to the rapid ^{1}H spin diffusion there. Under this situation, the

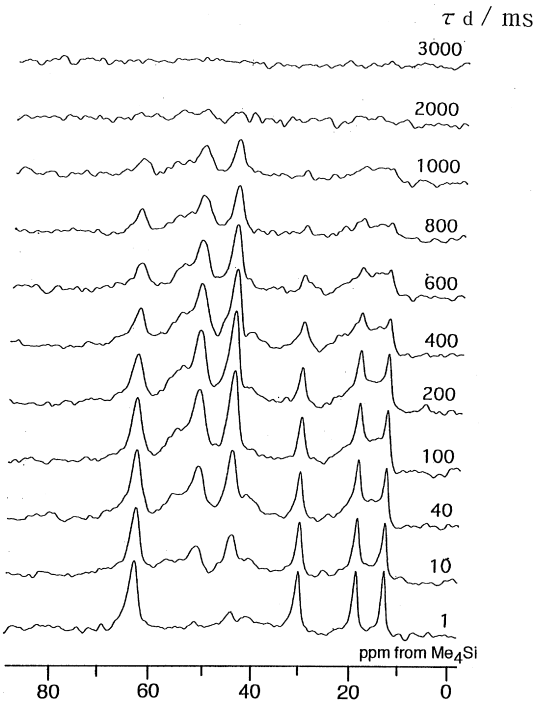

Fig. 4. ^{1}H spin diffusion process from the rubbery component (PBA) to the glassy component (PMMA) measured for BM at 30°C by the pulse sequence shown in Fig. 3.

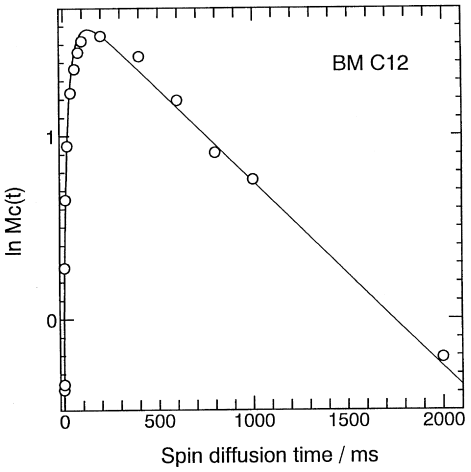

Fig. 5. Semilogaridimic plot for the peak intensity of the C12 resonance line shown in Fig. 4 as a function of the spin diffusion time τ_d. The solid line is the result simulated by Eq. (4).

time changes of the magnetizations M_R and M_G for PBA and PMMA are respectively given by simultaneous linear differential equations on the basis of the treatment of the two-spin system as follows:

$$dM_R/dt = (M_R - M_{Req}), \quad T_{1HR} - (M_R - M_G)/T_{SD} \tag{2}$$

$$dM_G/dt = (M_G - M_{Geq}), \quad T_{1HG} + (M_R - M_G)/T_{SD} \tag{3}$$

Here, M_{Req} and M_{Geq} are the thermal equilibrium magnetizations of the corresponding components. Under the usual experimental condition T_{SD} is assumed to be much shorter than T_{1HR} and T_{1HG}.

Moreover, it is also assumed that T_{1HR} and T_{1HG} are the same as a result of the rapid spin diffusion; $T_{1HR} = T_{1HG} = T_{1H}$. When these equations are solved under the initial condition of $M_R = M_{R0}$ and $M_G = M_{G0}$ at $t = 0$, the ^{1}H magnetization of the PMMA domains is described as follows:

$$M_G = (M_{R0} + M_{G0})\exp(-t/T_{1H}) - (M_{R0} - M_{G0})\exp(-2t/T_{SD}) \tag{4}$$

This equation is very similar to Eq. (1) describing the CP process. The solid line shown in Fig. 5 is the result simulated by Eq. (4). The experimental points agree well with the simulated curve obtained by the computer-aided least squares method. Similar good fitting was also obtained for samples BA1M and BA2M.

Table 5 lists the parameters appearing in Eq. (4) determined for the three samples. Since the ^{1}H magnetization of PMMA was suppressed by using the Goldman–Shen pulse sequence, M_{G0} is much smaller than M_{R0}. As is clearly seen, the T_{SD} value significantly depends on the concentration of the crosslinking agent; the T_{SD} value is the maximum for the BA1M. Since the larger TSD value represents the slower spin-diffusion, sample BA1M has smaller contact areas between PBA and PMMA domains. This fact suggests that the better phase-separated core-shell type structure may be formed in sample BA1M.

It is interesting to point out that the employment of an appropriate amount of the crosslinking agent seems to promote the core-shell type phase separation in this reaction system. This is not a strange thing in this system, because crosslinking is thought to preferentially occur at the first polymerization step of the core monomer at a rather low concentration of the crosslinking agent AMA and this leads to the reduction in the extent of the mixing of PBA with PMMA. In contrast, with increasing AMA concentration, some unreacted ally groups of AMA may be associated with the second polymerization of MMA, resulting in the higher extent of mixing between PBA and PMMA due to the crosslinking between them through the AMA residues. The formation of the better phase-separated structure in sample BA1M is also supported by the separate experimental result that this sample has the highest addition effect on the improvement of the impact strength for thermoplastic resins [32].

On the basis of these results, schematic structure models for the core-shell type polymer particles are shown in Fig. 7. As is shown in this figure, the polymer particles used in this work have not a typical core-shell type structure, but a rather incompletely phase-separated structure in which smaller PMMA domains are dispersed in the continuous PBA phase. The addition of an appropriate amount of the crosslinking agent AMA will confirm the distribution of the dispersed PMMA domains around the surface of the particles, probably by the preferential occurrence of crosslinking in the PBA phase as described above. Somewhat different structural models were also proposed for core-shell type polymer particles on the basis of detailed solid-state ^{13}C n.m.r. analyses [25–27]. It is, however, difficult to compare

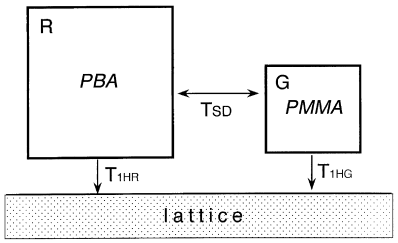

Fig. 6. Schematic representation for the energy exchange process in the ^{1}H spin systems of PBA and PMMA including the lattice.

Table 5
Time constants (T_{SD}) for the ^{1}H spin diffusion between the core and shell components, ^{1}H spin–lattice relaxation times (T_{1H}), and coefficients (M_{R0} and M_{G0}) appearing in Eq. (4) for the C12 carbon of PMMA, measured at 30°C

	BM	BA1M	BA2M
M_{R0}	5.7	4.6	2.3
M_{G0}	0.39	0.51	0.30
T_{SD} (ms)	25	32	28
T_{1H} (ms)	900	960	1000

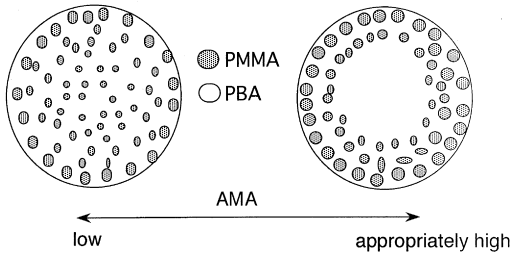

Fig. 7. Schematic representation of the phase-separated structure for the core-shell type polymer particles examined in this work.

our results with those previous results at present because the polymerization conditions are considerably different from each other.

4. Conclusions

The phase-separated structure for the core-shell type polymer particles, prepared by the two-step emulsion polymerization of BA and MMA in the presence or absence of the crosslinking agent AMA has been characterized by high-resolution solid-state ^{13}C n.m.r. spectroscopy and the following conclusions have been obtained:

1. The time constant T_{CH} for the cross polarization between ^{1}H and ^{13}C spin systems is found to be very sensitive for molecular mobility of crosslinked PBA in the rubbery state, whereas the spin-lattice relaxation times T_{1C} are almost insensitive for the crosslinking in those polymer particles. Sample BA2M, including 1.6 wt% AMA, is significantly restricted in molecular motion for the main-chain carbons of PBA and the side-chain carbon most closely connected to them.
2. The ^{1}H spin–lattice relaxation times ($T_{1\rho H}$) and the ^{13}C spin–lattice relaxation times ($T_{1\rho C}$) in the rotating frame measured at $-40°C$ have revealed that the PBA and PMMA phases are phase-separated in a scale of several nm instead of the typical core-shell type structure.
3. The ^{1}H spin diffusion process, which was measured for each sample at 30°C by the pulse sequence composed of the Goldman–Shen pulse sequence and the CP process, has been analyzed in terms of the equation derived by the simple two-spin cross relaxation theory. As a result, the time constant T_{SD}, which determines the ^{1}H spin diffusion rate between two polymer components, has been obtained for each sample. It has been found that this parameter is useful for the characterization of the phase separation of core-shell type polymer particles.
4. The polymer particles examined in this work do not have a typical core-shell type phase-separated structure but a rather incompletely phase-separated structure in which small PMMA domains are dispersed in the continuous PBA phase. However, the addition of an appropriate amount of the crosslinking agent AMA improves such a phase-separated structure by confining the distribution of the PMMA domains around the surface of the polymer particles probably as a result of the preferential crosslinking in the PBA phase.

References

[1] Nakamura Y, Ohta M, Okubo M. J Adhesion Soc, Japan 1996;32:104.
[2] Oshima J, Fujii T, Tachibana S, Tanaka M. Polym Prepr, Japan 1993;42:4665.
[3] Nelliappan V, El-Aasser MS, Klein A, Danniels ES, Roberts JE, Person RA. J Appl Polym Sci 1997;60:581.
[4] Nakamura Y, Tabata H, Okubo M, Matsumoto T. J Appl Polym Sci 1986;32:4865.
[5] Nakamura Y, Tabata H, Okubo M, Matsumoto T. J Appl Polym Sci 1987;33:885.
[6] Segall I, Dimonie MS, El-Aasser MS, Soskey PR, Mylonakis SG. J Appl Polym Sci 1995;58:385.
[7] O'Connor M, Tsaur S. J Appl Polym Sci 1987;33:2207.
[8] Arora A, Daniels ES, El-Aasser MS. J Appl Polym Sci 1995;58:301.
[9] Segall I, Dimonie VL, El-Aasser MS, Soskey PR, Mylonakis SG. J Appl Polym Sci 1995;58:401.
[10] Merkel MP, Dimonie VL, El-Aasser MS, Vanderhoff JW. J Appl Polym Sci Polym Chem Ed 1987;25:1755.
[11] Dickie RA, Cheung M, Newman S. J Appl Polym Sci 1973;17:65.
[12] Arora A, Daniels ES, El-Aasser MS, Simmons GW, Miller A. J Appl Polym Polym Sci 1995;58:313.
[13] Min TI, Klein S, El-Aasser MS, Vanderhoff JW. J Polym Sci Polym Chem Ed 1983;21:2845.
[14] Garcia-Rejon A, Rios L, Lopez-Latorre A. Polym Eng Sci 1987;27:463.
[15] Murou S, Hashimoto H, Hosoi K. Polym Eng Sci 1987;27:463.
[16] Schmidt-Rohr K, Spiess HW. Multidimensional solid-state NMR and polymers. London: Academic Press, 1994.
[17] Blumich B, editor. NMR basic principles and progress solid-state NMR III organic matter. Berlin: Springer, 1994.
[18] Tycho R, editor. Nuclear magnetic resonance probes of molecular dynamics. Dordrecht: Kluwer, 1994.
[19] Bovey FA, Mirau PA. NMR of polymers. London: Academic Press, 1996.
[20] Kuwabara K, Kaji H, Horii F, Bassett DC, Olley RH. Macromolecules 1997;30:7516.
[21] Kaji H, Horii F. Macromolecules 1997;30:5791.
[22] Ishida H, Kaji H, Horii F. Macromolecules 1997;30:5799.
[23] Ishida M, Yoshinaga IC, Horii F. Macromolecules 1996;29:8824.
[24] Egawa Y, Imanishi S, Matsumoto A, Horii F. Polymer 1996;37:5569.
[25] Landfester K, Boeffel C, Lambla M, Spiess HW. Macromol Symp 1995;92:109.
[26] Spiegel S, Landfester K, Lieser G, Beffel C, Spiess HW. Macromol Chem Phys 1995;196:985.
[27] Landfester K, Boeffel C, Lambla M, Spiess HW. Macromolecules 1996;29:5972.
[28] Opella SJ, Fery MHJ. J Am Chem Soc 1979;101:5854.
[29] Torchia DA. J Magnet Reson 1981;44:117.
[30] McArthur DA, Hahn ED, Walstedt RE. Phys Rev 1969;188:609.
[31] Horii F, Hu S, Odani H, Kitamaru R. Polymer 1992;33:2299.
[32] Oshima J, Ishida M, Morita H. Kobunshi Ronbunshu 1995;52:24.
[33] Goldman M, Shen L. Phys Rev 1966;144:321.